INTERNATIONAL JOURNAL FOR NUMERICAL METHODS IN FLUIDS
Int. J. Numer. Meth. Fluids 2004; **45**:109–123 (DOI: 10.1002/fld.489)

Numerical simulations of large falling drops

Louis Gottesdiener*,†, Denis Gueyffier, Mohammed Abdelouahab, Renée Gatignol and Stéphane Zaleski

Laboratoire de Modélisation en Mécanique, UMR CNRS 7607, Université Pierre et Marie Curie, 4, place Jussieu, 75252 Paris Cedex 05, France

SUMMARY

The numerical simulation in a two-phase medium of falling drops allows their velocities and shapes during the fall to be calculated. The terminal velocities and shapes for bromoform and chlorobenzene drops falling into water have been obtained. Although the method used calculates the flow inside and around the drop, it has not been possible to give results independent of the spatial discretization and the boundary effects. However, taking these influences into account, the numerical results agree with the experimental data given and the study consists of a good validation of the SURFER code used.

KEY WORDS: drop; falling drop; terminal velocity; two-phase medium; numerical simulation; fluid dynamic

1. INTRODUCTION

Thanks to experimental observations, it is well known that under the effect of gravity a drop of liquid, which is at first spherical and stationary, placed in another non-mixable liquid, ends up falling—if it does not break down beforehand—at a constant velocity called the terminal velocity with a constant shape called the terminal shape. This velocity and shape depends, among other parameters, on the initial diameter of the drop. The expression 'equivalent spherical diameter' often encountered in literature refers to the diameter of a sphere having the same volume as the deformed drop, which, in our case, means the initial diameter.

With regard to the fall of a drop, initially spherical and dropped in a liquid or a gaseous fluid at rest, we can distinguish many zones according to the type of deformation reached by the drop (Figure 1). At the beginning of the fall, there is a first zone, called the initial zone, where the drop reaches its terminal velocity almost like a solid rigid sphere. The second zone is where the drop reaches its maximum terminal velocity called limit velocity at the summit of the velocity peak. This zone is called the limit zone. A third zone is the transition zone

* Correspondence to: L. Gottesdiener, 17 Av. Dr. Arnold Netter, 75012 Paris, France.
† E-mail: helenelouis@wanadoo.fr

Received 1 March 2001
Revised 10 August 2002

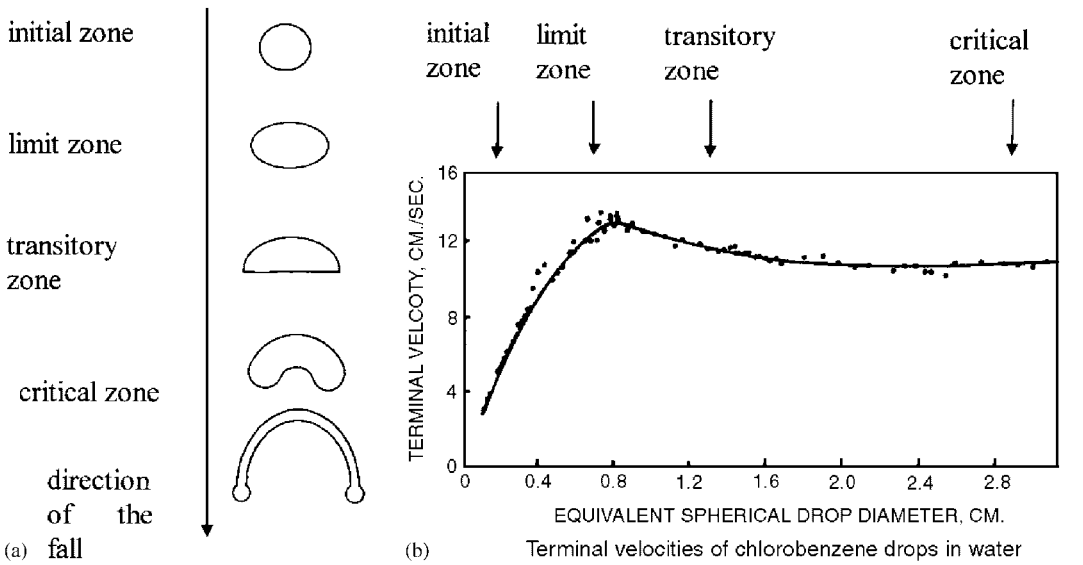

Figure 1. Shapes and zones during the fall: (a) extract of [1]; (b) extract of [3].

in which the terminal velocity diminishes slightly. Finally we have the fourth zone called the critical zone where the drop reaches its critical terminal velocity before it crumbles. The observation of the drop silhouette leads towards the illustration given in 1(a) taken from Reference [1] where the parachute shape in the critical zone was observed for big drops of chloroform falling in sugared water [2]. These different zones are presented in Figure 1(b) taken from Reference [3] in the case of chlorobenzene drops falling into water where the experimental terminal velocity is expressed according to the equivalent spherical diameter.

Although the experimental means enabled the observation of the drop's fall under the effects of gravity early on, it is only recently that numerical codes have succeeded in simulating it in a satisfactory manner. A vectorized code called SURFER has been developed by S. Zaleski and his team [4, 5] allowing them to simulate the deformation of a drop placed in an initially uniform flow by using either the axisymmetrical or the three-dimensional code version. In one of its first versions, the latter (called cubic in the rest of the text) enabled the initialization of a drop which falls under the effect of gravity, in a cubic box (measuring CGS: $1\text{ cm} \times 1\text{ cm} \times 1\text{ cm}$). Using periodic boundary conditions on some faces opposing each other, the fluid going out from one side is reintroduced into the other. Thus the drop which disappears from one side reappears on the other, in such a way that the trajectory is split up into a succession of periodic passages across the box. This allows calculations to be made with more or less refined spatial definitions (number of cells equal to 34^3 or 66^3 or 128^3) in the box using a moderate computer space memory. However, the drop falls in its proper wake so that a series of three-dimensional equidistant drops are so simulated. Thus one must take into account the interaction between drops in the interpretation of the results. The wake effect, recently studied for two drops interacting [6], has been evaluated as negligible but the existence of drops not only above or below but also laterally renders our situation more complex and more sensitive to interactions.

At every time step and in every cell of the box, the code calculates the velocity field relative to a referential frame attached to the centre of gravity of all the fluid in the box. Then the drop fall velocity calculated versus a fixed referential frame can be deduced [7, 8]. As the code follows the interface between the discrete and dispersed phases during the stage of deformation, it also allows the shape taken by the drop to be described up to its terminal velocity during the fall [9, 10].

The purpose of this article is to validate the SURFER code by comparing the numerical terminal velocities and shapes to the experimental ones, in concrete cases of non-miscible liquids moving in the box.

2. THE COMPUTATION DOMAIN

As it has been mentioned earlier, the way the drop deforms its terminal velocity is influenced by factors such as the proximity of the edges and the boundary conditions of the computation domain. Furthermore, we can select between the mirror boundary conditions and the boundary conditions of periodicity. When we apply a mirror condition on one side, the fluid slides onto it without going through, thus simulating the presence of a wall, whereas for a condition of periodicity on a side, the fluid goes through it and it is the presence of a neighbouring flow which is simulated. The results of a numerical calculation are generally valid only if there is absolutely no influence of numerical parameters such as spatial and temporal discretization. This independence having not been attained because of computing time costs involved by the choice of a too large box size, this is their influence on the results which are presented and discussed next.

2.1. The cubic domain

The calculation domain consists of a cube whose edges are arranged according to the axis x, y, z of a Cartesian frame attached to the centre of gravity of all the fluid contained in the cube, x being the fall direction. We cut the edges directed according to x, y and z into nx, ny and nz segments respectively, with $nx = ny = nz$ in the cubic case. The cube is characterised by the length L of an edge (Figure 2). Thus the numeric domain is uniformly decomposed into cubic cells of size h^3, where $h = L/nx$ is the space step which characterizes the spatial definition or discretization of the domain.

The boundary conditions used in this domain are conditions of periodicity on the superior and inferior sides crossed by the drop when it falls, as well as the two vertical sides which are opposite to each other. On the other two vertical remaining sides we use mirror conditions. Such a configuration enables the influence of different boundary conditions to be compared but introduces a dissymmetry between the vertical sides of the domain, which is not realistic regarding to the experimental situation. If D is the initial drop diameter, D/h represents its initial discretization.

The numerical treatment of the fall appears to be dependent not only on the parameter D/h but also on parameter L/D. In fact this latter proportion determines the closeness of the edges with regard to the drop and their influence on its deformation. Moreover we must take into consideration, by limiting L/D, the maximum spread the drop takes while deforming a lot, because it risks touching the edges during the calculation. Obviously the ideal situation

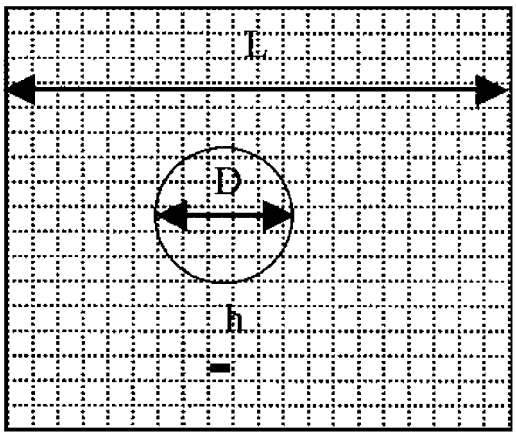

Figure 2. The cubic calculation domain.

to avoid all these influences would be to push back the edges far enough to maintain a uniform environment far from the drop—which would reproduce the experimental conditions at best—while maintaining an accurate spatial definition. This cannot currently be envisaged, as it would be very costly in computing time, as previously noted.

Thus, we are looking to have large values of D/h and L/D simultaneously. This leads to small values of h for a given drop diameter D and we come across the following contradiction:

- On the one hand, introducing a large drop into a small area leads to good drop definition and good quality for interface calculations but there is also a strong edge influence on the drop.
- On the other hand, pushing away the edges of the area to reduce their influence on the drop results in increasing the computational area. In order to avoid taking up too much computer memory space and calculation time, we must reduce the spatial definition which causes detriment to the discretization and thus to the precision of the calculation.

These contradictory elements feed the discussion which will arise when presenting the results and are valid for the different areas of calculation and the various code versions.

It must be noted that for values of nx superior to 66, the use of a super-computer—of the CRAY type, for example—is necessary.

2.2. *Parallelepipedal area*

In this type of area different values of nx, ny and nz can be chosen. As indicated above, the advantage of this version is to reduce the influence of the wake on the terminal velocity considering $L = 2$ or 3 cm for example in the direction of the fall while restraining the size of the other two dimensions of the area. For this case, boundary conditions of periodicity have been used on every side preserving the symmetrical aspect of the numerical treatment. The evolution of the drop during the fall appears more likely considering that the trajectory generally stays closer to the vertical and the shape achieved by the drop after deformation presents a more axisymmetrical appearance according to the vertical direction. In directions

y and z, the sizes are defined by $h.ny$ and $h.nz$ with $nx = 130$, $ny = nz = 66$. Thus while $L = 1$ cm in the nx direction, the size in the others is only 0.5 cm and the effects of the edges are more sensitive.

As it has already been noted, while the drops are relatively large compared with the area and are being deformed a lot, they run the risk of touching the edges. To avoid this, L has been increased sufficiently in proportion to the initial drop diameter. On the contrary while the drops are relatively small for a fixed number nx, it would seem appropriate to reduce L with regard to the initial drop diameter, otherwise the spatial definition risks being insufficient.

2.3. Axisymmetrical domain

An axisymmetrical version of the code was available. In this case L represents the maximum radial dimension of the domain. This version needs far less calculation time than the three-dimensional versions. This could be easily used on less powerful computers (PC, RS6000 stations, etc.) than the CRAY computers. It allows the setting up of a larger computational area while preserving good spatial definition. It does not, however, allow the appearance of trajectory deviation (or zigzagging) during the fall—which is sometimes characteristic of some liquids—and more generally of all three-dimensional aspects.

Finally it can be seen that regardless of the areas of calculation under consideration, they do not avoid the wake effect. This is an inherent drawback to the method, so we cannot hope for better than reducing its influence, to a greater or lesser extent, by taking an area much larger than the size of a drop while preserving good spatial definition. Thus the ideal case would correspond to the largest possible values of both D/h and L/D, which is almost only possible for the axisymmetrical area. The drop in this case however, has to stay in the vertical fall direction. This restriction is not realistic in some cases where it may be responsible for fluctuations, which appear in the fall velocity, as we shall see in the following.

3. RESULTS AND DISCUSSIONS

Among a large variety of fluid combinations experimented upon in two-stage experiments, we have come to rest on the case of drops falling in the water, made of either chlorobenzene or bromoform. The reason for this is that the former material deforms very little and the latter deforms a lot. This choice was made taking into account the known experimental results.

3.1. The terminal velocities

As the numerical codes calculate the fluid velocity in each cell of the calculation area, the average drop velocity can be determined at any moment. Two cases can be observed concerning this velocity: either it regularly tends towards a boundary value constant in the time and the terminal velocity is determined by this constant, or it begins fluctuating with time and no constant limit is clearly defined. In this latter case which appears the most frequently, the first maximum of this average velocity has been systematically taken as terminal velocity value.

Figures 3 and 4 sum up the results concerning the drops of chlorobenzene and bromoform respectively. The tables in Figures 3 and 4 present the numerical parameters which characterize the studied cases either in three-dimensional geometry (named num-3d) or in axisymmetrical

Table I

D (mm)	nx	ny	nz	L (cm)	h	L/D	D/h	$V_{t\,num}$	$V_{t\,exp}$	Δ
num-3c										
1	130	66	66	0.6	0.005	6	21.3	5	2.9	0.72
1	130	66	66	0.8	0.006	8	16	4	2.9	0.38
1	130	66	66	1	0.008	10	12.8	3.09	2.9	0.07
2	130	66	66	0.8	0.006	4	32	6.85	5.5	0.25
2	66	66	66	1	0.016	5	12.8	9.5	5.5	0.73
2	130	66	66	1	0.008	5	25.6	7.46	5.5	0.36
3	66	66	66	1	0.016	3.33	19.2	6.2	7.8	-0.2
3	66	66	66	2	0.031	6.67	9.6	7.82	7.8	0
4	130	66	66	2	0.016	5	25.6	9.37	9	0.04
5	66	66	66	1	0.016	2	32	8	10.5	-0.2
5	66	66	66	2	0.031	4	16	10.1	10.5	-0
6	66	66	66	1	0.016	1.67	38.4	7.5	11.5	-0.3
6	130	66	66	2	0.016	3.33	38.4	9.05	11.5	-0.2
8	130	66	66	4	0.031	5	25.6	10.91	13	-0.2
num-axi										
1	514	130		0.1	8E-04	1	128	4	2.9	0.38
1	514	130		0.2	0.002	2	64	5.3	2.9	0.83
1.5	514	130		0.2	0.002	1.33	96	5.6	4.25	0.32
2	514	130		0.2	0.002	1	128	9.6	5.5	0.75
2	514	130		0.3	0.002	1.5	85.3	10.04	5.5	0.83
3	514	130		0.3	0.002	1	128	10.97	7.8	0.41
3	514	258		0.3	0.001	1	256	13.9	7.8	0.78
4	514	130		0.5	0.004	1.25	102	11.7	9	0.3
4	514	130		1	0.008	2.5	51.2	10.64	9	0.18
5	514	130		1	0.008	2	64	11.22	10.5	0.07
5	514	130		2	0.016	4	32	14.04	10.5	0.34
6	514	130		0.5	0.004	0.83	154	10.4	11.5	-0.1
6	514	130		2	0.016	3.33	38.4	14.04	11.5	0.22
8	514	66		1	0.016	1.25	51.2	10.8	13	-0.2
8	514	130		1	0.008	1.25	102	11.7	13	-0.1
10	514	130		1	0.008	1	128	9.5	12.5	-0.2
10	514	130		2	0.016	2	64	10.93	12.5	-0.1

(a)

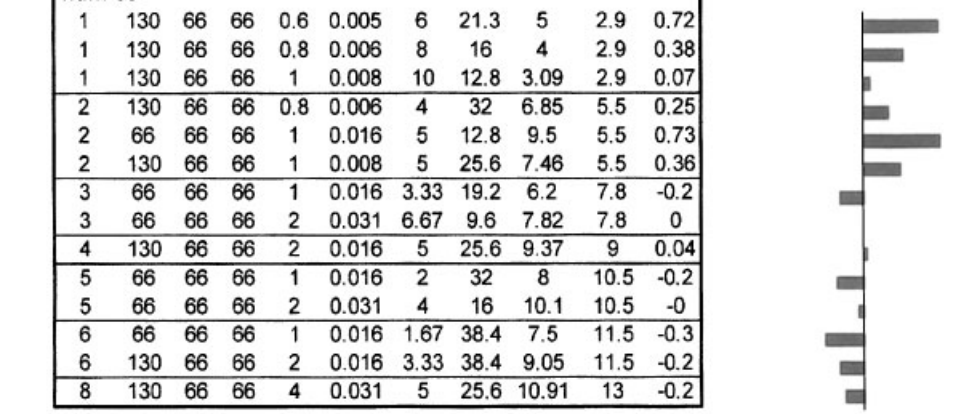

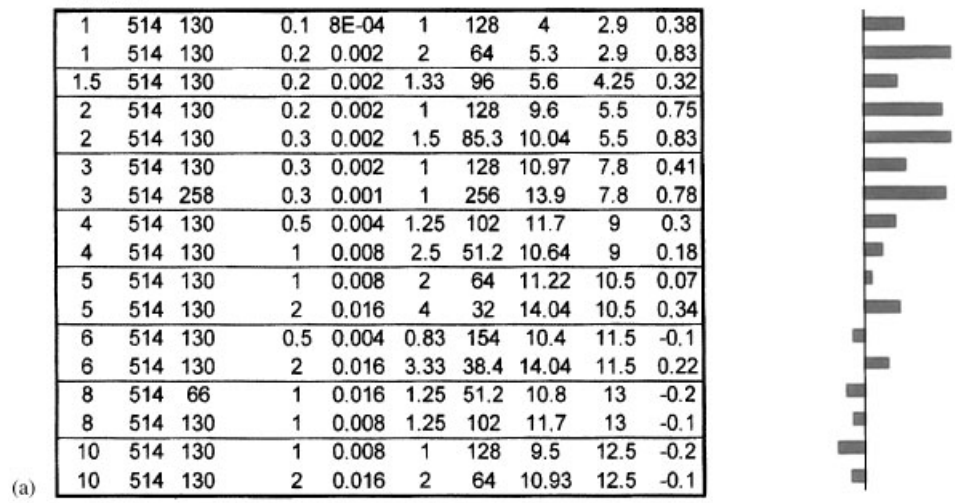

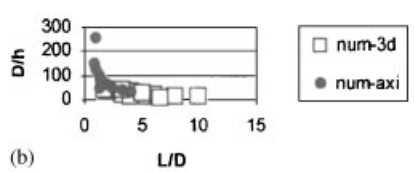

(b)

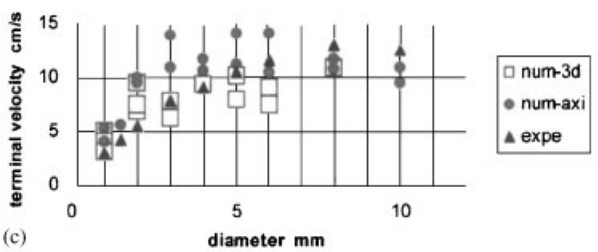

(c)

Figure 3. Chlorobenzene drops fall in water: (a) $\Delta=(V_{t\,num}-V_{t\,expe})/V_{t\,expe}$: (b) Discretisation/proportion; (c) Terminal velocity: Chlorobenzene.

Table I

D (mm)	nx	ny	nz	L (cm)	h	L/D	D/h	$V_{t\,num}$	$V_{t\,exp}$	Δ
num-3c										
1	66	66	66	1	0.02	10	6.4	14.6	18.5	-0.2
1	130	66	66	0.8	0.01	8	16	35.9	18.5	0.94
1	130	66	66	1	0.01	10	12.8	30.6	18.5	0.65
1	130	66	66	1.2	0.01	12	10.7	27	18.5	0.46
1	130	66	66	1.6	0.01	16	8	21.3	18.5	0.15
2	66	66	66	1	0.02	5	12.8	28.4	23.9	0.19
2	130	66	66	1	0.01	5	25.6	25.6	23.9	0.07
2	130	66	66	2	0.02	10	12.8	28	23.9	0.17
3	130	66	66	2	0.02	6.67	19.2	22.1	22.6	-0
4	130	66	66	2	0.02	5	25.6	18.8	22.3	-0.2
4	130	66	66	3	0.02	7.5	17.1	19.95	22.3	-0.1
5	130	66	66	2	0.02	4	32	18	22.3	-0.2
5	130	66	66	3	0.02	6	21.3	20.1	22.3	-0.1
6	130	66	66	2	0.02	3.33	38.4	17.1		
6	130	66	66	3	0.02	5	25.6	20.7		
num-axi										
1	514	130		0.2	0	2	64	33.5	18.5	0.81
1	514	258		0.2	0	2	128	32.1	18.5	0.74
1	514	258		1	0	10	25.6	34	18.5	0.84
2	514	258		0.3	0	1.5	171	29.3	23.9	0.23
2	514	130		0.4	0	2	64	35	23.9	0.46
2	514	258		1	0	5	51.2	26.2	23.9	0.1
4	514	66		1	0.02	2.5	25.6	20.15	22.3	-0.1
4	514	130		1	0.01	2.5	51.2	20.8	22.3	-0.1
4	514	258		1	0	2.5	102	22.8	22.3	0.02
5	514	258		1	0	2	128	21.3	22.3	-0
5	514	130		2	0.02	4	32	20.6	22.3	-0.1

(a)

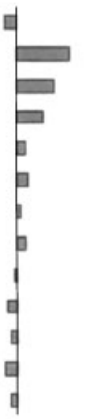

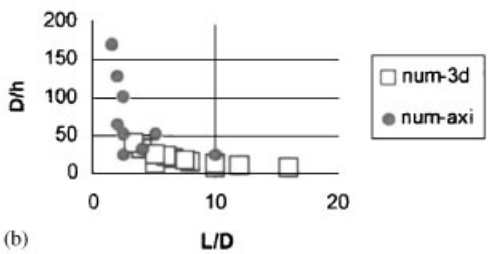

(b)

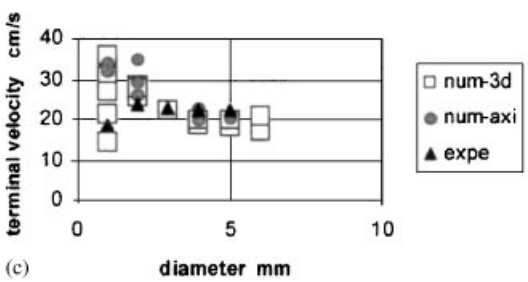

(c)

Figure 4. Bromoform drops fall in water: (a) $\Delta = (V_{t\,num} - V_{t\,expe})/V_{t\,expe}$; (b) Discretisation/proportion; (c) Terminal velocity: bromoform.

geometry (named num-axi) as well as the numerical results for the terminal velocity. In the part num-3d of the charts, the distinction between the cubic and parallelepipedal domains is shown by the values taken by *nx*, *ny* and *nz*, but it does not appear on the curves where these cases are represented by the same sort of squares. The quantity called Δ (Figures 3(a) and 4(a)) measures the relative gap between calculation and experiment and is obtained by the relation: $\Delta = (V_{\text{t num}} - V_{\text{t expe}})/V_{\text{t expe}}$ where $V_{\text{t num}}$ and $V_{\text{t expe}}$ are the vertical components of the terminal velocity in the numerical and experimental cases respectively. The $V_{\text{t expe}}$ values are taken from Reference [3]. The variations of the discretization D/h and the proportion L/D are presented in Figures 3(b) and 4(b). The terminal velocity values calculated with different codes for different drop diameters are compared with each other and with experimental values (Figures 3(c) and 4(c)) as well. The numerical parameter's influence is also shown insofar as the terminal velocity takes different values for the same diameter and a given code version.

3.1.1. Comparison with experiment. In a general manner, despite a certain scattering of results, it has always been possible, varying the discretization D/h and the proportion L/D, to bring together the values of the numerical terminal velocity and the experimental ones (Figures 3(c) and 4(c)) and these values also present a scattering around the average line (Figure 1b). It appears that on this point, the two code versions have their own advantages and drawbacks. Thus, in num-axi, one can reach drop discretization D/h far superior, up to 5 times and more than in num-3d (Figures 3(b) and 4(b)). However the terminal velocity obtained is not closer to the experiment. This leads to the understanding that, concerning the terminal velocity, the spatial definition D/h is not necessarily preponderant regarding the effects of the edge which find itself introduced or amplified for weak L/D values.

The spatial definition influence in num-axi can be clearly shown as in the case of the 4 mm drop of bromoform (Figure 4(a)). While *nx* value is refined from 66 to 130 and then to 258, the gap with the experiment is reduced by 10–7% then 2%, everything being equal otherwise.

Moreover it can be noticed that it is not always by increasing the discretization D/h—as it could have been thought at first—that this bringing together could be achieved, sometimes by increasing the proportion L/D (Figures 3(a) and 4(a)). Thus, in num-axi, if it is correct for the 6 mm drop of chlorobenzene, it is not the case for the 4 mm or the 10 mm drop. In the same manner, in num-3d, if it applies to the 2 mm drop of bromoform, it doesn't apply to that of 5 mm or 1 mm drops. This reveals that the role and relative importance of the two parameters L/D and D/h can be inverted according to the situations considered: in spite of a good discretization, the drop can suffer from a strong influence on the edges. Inversely we can get closer to the experiment by widening the edges but this will be to the detriment of the discretization.

Generally, on the one hand, the results are dependent on the numerical parameters, and on the other, the velocity values obtained are of the order of magnitude of the experimental values. Thus it can be concluded that:

- the phenomenon of the fall is correctly treated by the code.
- it is only in terms of the precision that the numerical parameter's influence on the terminal velocity appears.
- a more rigorous confrontation with the experiments would need to render the calculations independent of discretization, which would actually be very expensive.

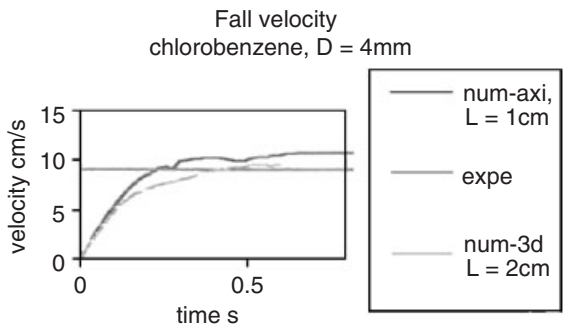

Figure 5. Fall velocity.

3.1.2. Comparisons between code versions. Despite the very good spatial definitions easily obtained by the axisymmetric version for reduced edge effects, it does not give very different results from those obtained by the three dimensional one. However the numerical parameters influence are not the same. For example the two versions treat the case of the 1 mm diameter drop in a similar way, the result for the chlorobenzene being relatively closer to the experiment than for the bromoform (Figures 3(c) and 4(c)). However, the roles of discretization D/h and proportion L/D are different in both cases. Thus, for the bromoform, in num-axi, the more realistic terminal velocity V_t value of 32.1 cm/s corresponds at the same time, to the best discretization ($D/h = 128$) and to very obvious edge effects ($L/D = 2$). On the other hand, in num-3d, this value is not reached for the best discretization ($D/h = 8$) but by reducing the edge effects as far as possible ($L/D = 16$). The same applies for the chlorobenzene. There is a tendency to conclude that the num-3d version is more sensitive to the edge effects than the num-axi version.

3.2. Fall time and initial acceleration

As previously noted, the curve $V(t)$ describing the change in velocity according to time since the initial moment highlights the point at which terminal velocity is attained. It simultaneously delivers the fall time—namely the time the drop takes to reach its terminal velocity—as well as the initial acceleration.

When it can be clearly defined, the fall time is comparable for the two code versions: for example, they give 0.4 s for the 4 mm chlorobenzene drop (Figure 5) or still 0.05 s for the 4 mm bromoform drop (Figure 6) as well as for the bromoform 5 mm one. These times are very short but concur with the remarks made by the experimenters who noted that terminal velocity may be reached very early after the release of the drop [2, p. 305].

The initial acceleration under gravity for the chlorobenzene (Figure 5) is $0.5\,\mathrm{m/s^2}$ for a drop of 4 mm diameter, a value very close to $0.6\,\mathrm{m/s^2}$ represented by the theoretical expression $g(\gamma - 1)/(\gamma + 0,5)$, where γ represents the density ratio and g the gravity acceleration [2]. The agreement is also good for the 4 mm bromoform drop (Figure 6) for which is obtained $5\,\mathrm{m/s^2}$, very close to the theoretical value of $5.42\,\mathrm{m/s^2}$.

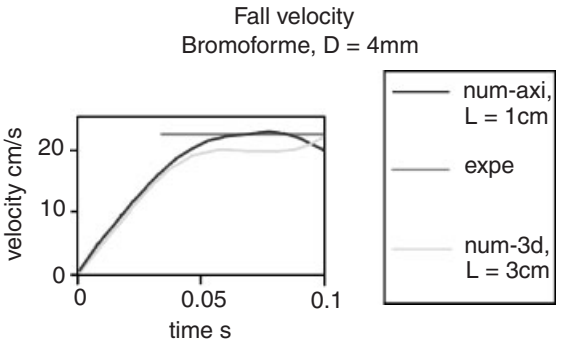

Figure 6. Fall velocity.

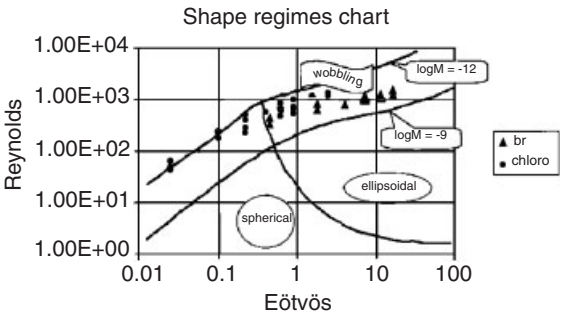

Figure 7. Shape regimes chart.

3.3. Study of shapes

Drops falling in free fall in infinite media under the influence of gravity are generally grouped under the following categories: (a) spherical, (b) ellipsoidal, (c) spherical-cap or ellipsoidal-cap. In the past [2], it has been possible to prepare a generalized graphical correlation—or shape regimes chart—based on experimental observations in terms of the following numbers: Eötvos number $Eo = g(\Delta\rho)d_e^2/\sigma$, Morton number $M = g\mu^4(\Delta\rho)/\rho^2\sigma^3$ and Reynolds number $Re = \rho d_e U/\mu$. In these relations μ is the dynamical viscosity and ρ is the density of the dispersed phase, σ is the interfacial tension, $\Delta\rho$ is the density difference between the two phases.

Other particular features associated with the fall can also be the subject of theoretical and experimental confrontations, such as the breaking and the oscillating frequency of the drops.

3.3.1. Shape regimes. Generally speaking, the ellipsoidal regime responds only to relatively weak Morton numbers ($M < 10$), while the spherical regime applies to all Morton numbers. With regard to the wobbling regime—namely when falling drops undergoing random wobbling motions—it corresponds to very low Morton numbers ($M \sim 10^{-12}$) and high Reynolds numbers ($Re \sim 10^3$) [2]. In Figure 7 (taken from the chart given in Reference [2]) the distribution of the various possible regimes is presented with the experimental separating lines. All the cases numerically studied for the bromoform (circles) and the chlorobenzene (triangles) are represented in it. For the cases considered, the Morton numbers are very low, between 10^{-9}

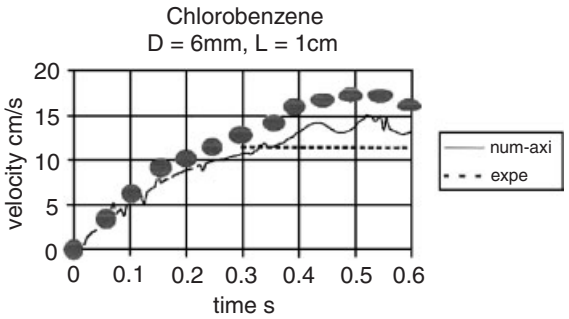

Figure 8. Falling drop deformations.

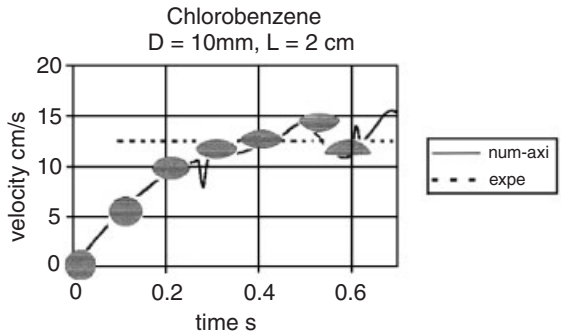

Figure 9. Falling drop deformations.

and 10^{-12}; thus, the regimes concerned go from the spherical to the wobbling regime, through to the ellipsoidal one (Figure 6). This compares reasonably favourably with the experimental chart, at least, if one focuses only on the beginning of the terminal velocity fall phase, considering that the presence of pulsations and other edges interactions interfere with the drop shape during the second part of the fall, as it will be seen next.

3.3.2. Shapes during the fall. The presentation of the drop profiles during the fall highlights two clearly distinct phases. The first extends from $t = 0$ to the time where the terminal velocity is well established, while the drop changes progressively from the spherical shape to the ellipsoidal or semi-ellipsoidal depending on the case. The second phase begins after this and can be described as the destabilization stage of the fall in terminal velocity state (see Figures 8 and 12). The shape fluctuates more or less between oblate and prolate, in phase with the velocity curve fluctuations.

These fluctuations or oscillations can come from the drop itself as the experiments have proved [2, p. 168; 3]. However in our numerical case it can also come from the presence of the wake in which the drop falls. An agreement with the experiment can be observed [3] for the spheroidal shape of the 6 and 10 mm chlorobenzene drops (Figures 8 and 9), and for 4 and 5 mm bromoform drops (Figures 10 and 12). On the other hand, the 2 mm drop of bromoform (Figure 11) is faraway from the spherical shape although the experiments [3] indicate that it remains spherical up to 3 mm in diameter.

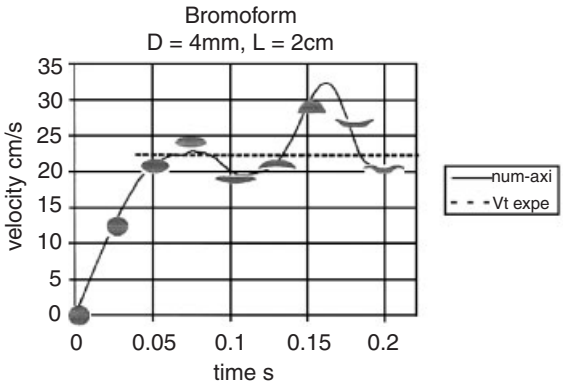

Figure 10. Falling drop deformations.

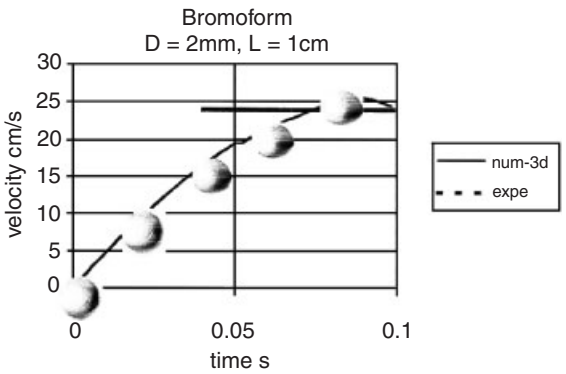

Figure 11. Falling drop deformations.

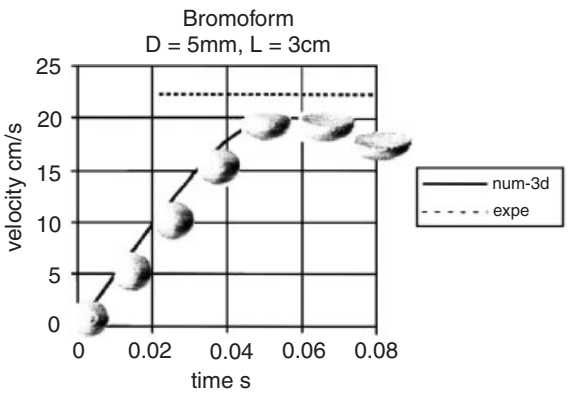

Figure 12. Falling drop deformations.

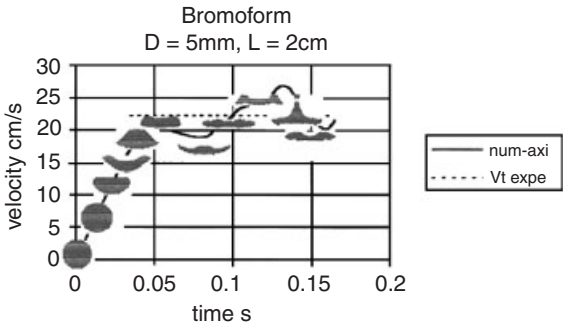

Figure 13. Drop breaking.

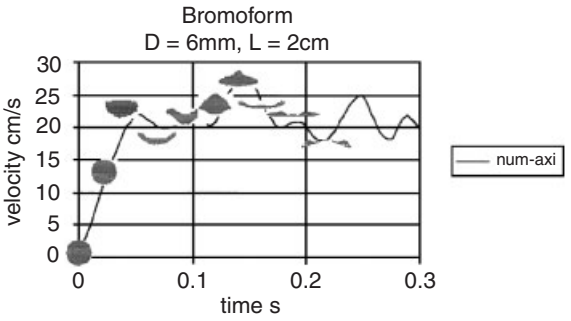

Figure 14. Drop breaking.

3.3.3. Drops breaking. The drops breaking is more easily reached using the axisymmetrical code version, which allows the falling drop to be followed for a sufficient period of time. Experiment [3] gives 5 mm as a maximum diameter value, for a bromoform drop falling in terminal velocity, before breaking. In agreement, calculations (Figures 13 and 14) confirm the breaking appearance for the 5 and 6 mm drops. It appears after a thickness reduction in the fluid film during the pulsation, when a satellite—namely a separation of a small part of the primary drop—is expulsed (Figure 13). The agreement between calculation and experiment on the drop breaking diameters in the case of bromoform reinforce the idea that oscillations may be a drop breaking mechanism while starting to interact with instabilities due to the drop wake, as it has been already suggested [2, p. 188]. In fact, the only way to study the drop breaking appearance numerically would be to remove the edge effects completely.

3.3.4. Frequency of oscillations. Among the secondary drop movements, the fluctuations have been analysed differently, according to the authors, from the Weber number or the Reynolds number [2, p. 185–187]. The very simplified model based on the drop's natural oscillation frequency enables a rough theoretical comparison to be made. The drop's natural oscillation frequency is given by [11]: $f_N = \sqrt{\frac{48\sigma}{\pi^2 d_e^3 \rho(2+3\gamma)}}$, where σ is the interfacial tension, d_e is the equivalent spherical diameter, ρ is the water density and γ is the density ratio. Figures 15 and 16 show the oscillations appearing during the 6 and 8 mm chlorobenzene drops' fall.

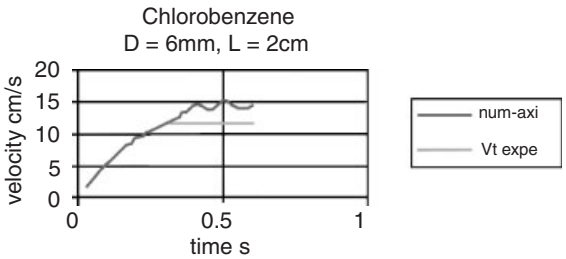

Figure 15. Velocity fall oscillations.

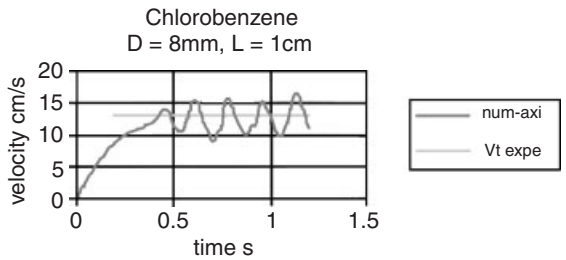

Figure 16. Velocity fall oscillations.

Frequencies of around 6 and 10 Hz have been detected relatively close to the 8.06 and 12.42 Hz theoretical values, for the 8 and 6 mm diameters, respectively.

As experiment [3] does not indicate any oscillation for the chlorobenzene drops falling in water, it can be attributed to the edge effect. In fact this is particularly evident because, for this 8 mm drop, the parameter L/D is equal to the relatively low value 1.25 (Figure 16). Moreover the amplitude of the oscillations are stronger here than for the 6 mm drop (Figure 15) for which the edge effects are lower because $L/D = 3.33$ in this case.

4. CONCLUSION

This study, putting the SURFER code into action in its three dimensional and axisymmetrical versions, allowed us to numerically determine the terminal velocity and shapes of drops falling into water. In the versions presented here, the code describes the drop's fall correctly, but cannot do it without the edge influence and consequently cannot be used for a precise quantitative validation through the terminal velocity. In fact these influences introduce oscillations which destabilize the fall, thus fluctuating the terminal velocity and shape of the drop.

Taking into account these restrictions, the agreement with the experiment stays good concerning the order of magnitude of the terminal velocity. Likewise the shape taken by the drops corresponds well to the regime predicted by the experimental correlations, at least during the installation phase of the fall in terminal velocity. Using the axisymmetrical code version, the breaking of the bromoform drop is produced for the diameter of 5 mm, in accordance with the experiment. The connection with theory is also relatively good as far as the initial acceleration and the pulsation during the fall are concerned.

The terminal velocity's calculation does not permit a clear preference to be distinguished between the axisymmetrical and three dimensional approaches for the treatment of the fall, as well as in the case of weak and strong deformations, in small as well as large diameters. The axisymmetrical code could however be preferable for the following reasons: it is more practical, less difficult to manipulate, it needs less calculation time and it is more easily adapted to a refinement of the spatial definition.

ACKNOWLEDGEMENT

The authors would like to thank IDRIS where calculations have been performed and are extremely grateful to the IDRIS support services.

REFERENCES

1. Abdelouahab M. Rapport post-doctoral, L.M.M., Université Paris VI, 1995.
2. Clift R, Grace JR, Weber ME. Bubbles, *Drops and Particles*, Ac. Press: 1978.
3. Krishna PM, Venkatesvarlu D, Narasimhamurti SR. Fall of Liquid Drops in Water. *Journal of Chemical and Engineering Data* 1959; **4**:336–344.
4. Lafaurie B, Nardone C, Scardovelli R, Zaleski S, Zanetti G. Modelling merging and fragmentation in multiphase Hows with SURFER. *Journal of Computational Physics* 1994; **113**:134–147.
5. Li J. Calcul d'interface affine par morceaux. *Comptes Rendus de l'Académie des Sciences de Paris Série B* 1995; **320**:391–396.
6. Paul SK. Velocities of water drops falling in oil media and the wake effect. *Indian Journal of Radio & Space Physics* 1999; **28**(1):15–21.
7. Gueyffier D. Rapport de DEA de Mécanique, L.M.M., Université Paris VI, 1996.
8. Olson JF, Rothman DH. Two-fluid flow in sedimentary rock: simulation, transport and complexity. *Journal of Fluid Mechanics* 1997; **341**:343–370.
9. Actes du 36ème Congrès de Mécanique, Faculté des Sciences de Tetouan, SMSM, 22–25 Avril 1997.
10. Actes du l3ème Congrès Français de Mécanique, Futuroscope, 1–5 Sept. 1997.
11. Lamb H. *Hydrodynamics* (6th edn). Cambridge Univ. Press: London, 1932.

